

Revisiting CMB constraints on Warm Inflation

Richa Arya,^a Arnab Dasgupta,^a Gaurav Goswami,^b Jayanti Prasad,^c Raghavan Rangarajan^a

^aTheoretical Physics Division, Physical Research Laboratory, Ahmedabad 380009, India

^bSchool of Engineering and Applied Science, Ahmedabad University, Ahmedabad 380009, India

^cInter-University Centre for Astronomy and Astrophysics, Pune 411007, India

E-mail: richaarya@prl.res.in, arnabd@prl.res.in, gaurav.goswami@ahduni.edu.in, jayanti@iucaa.ernet.in, raghavan@prl.res.in

Abstract. We revisit the constraints that Planck 2015 temperature, polarization and lensing data impose on the parameters of warm inflation. To this end, we study warm inflation driven by a single scalar field with a quartic self interaction potential in the weak dissipative regime. We analyse the effect of the parameters of warm inflation, namely, the inflaton self coupling λ and the inflaton dissipation parameter Q_P on the CMB angular power spectrum. We constrain λ and Q_P for 50 and 60 number of e-foldings with the full Planck 2015 data (TT, TE, EE + lowP and lensing) by performing a Markov-Chain Monte Carlo analysis using the publicly available code `CosmoMC` and obtain the joint as well as marginalized distributions of those parameters. We present our results in the form of mean and 68 % confidence limits on the parameters and also highlight the degeneracy between λ and Q_P in our analysis. From this analysis we show how warm inflation parameters can be well constrained using the Planck 2015 data.

Contents

1	Introduction	1
2	Evolution equations in warm inflation	3
3	Warm inflation model with a quartic potential	5
3.1	The primordial power spectrum	5
3.2	Obtaining the dissipation parameter Q_k	6
3.3	Duration of inflation	7
4	Primary analysis using the primordial power spectrum and its normalisation	9
4.1	Spectral index	9
4.2	Coupling parameters λ and C_ϕ as a function of Q_P	11
4.3	Thermal equilibrium and a lower bound on Q_P	13
4.4	Correlation between λ and Q_P	13
5	Analysis of the effects of warm inflation parameters on the CMB angular power spectrum	14
5.1	λ and Q_P	14
5.2	Effect of the <i>coth</i> term, and a comparison with cold inflation	14
5.2.1	Recovering cold inflation	16
6	Comparison with the existing literature	16
7	Constraining the parameters of the warm quartic chaotic inflation model with the full Planck 2015 data	17
8	Discussion and Conclusions	20

1 Introduction

Cosmic inflation [1–9] is a phase of accelerated expansion in the early history of the Universe during which the energy density of the Universe is dominated by the density of a slowly rolling scalar field, the inflaton. In the simplest models of this inflationary paradigm, it is assumed that the number density of all the particles becomes negligible during inflation due to which slow roll inflation occurs in an almost perfect vacuum state. The inflaton field is coupled to other fields so that it may dissipate its energy after inflation and reheat the universe. However one may consider the possibility that dissipative effects are important not only after but also *during* the slow-roll phase of inflation. In that case, under appropriate conditions, there is a thermal bath present during the accelerated expansion also, and if the temperature of the bath is greater than the Hubble parameter H , then this scenario is known as *Warm Inflation* [10–12](see Ref. [13] for a more recent discussion on dissipation during inflation).

Why should one consider warm inflation? Firstly, it is natural to consider inflaton couplings not just during reheating but also during inflation. Furthermore, for some warm

inflation models, the eta problem, namely, the presence of large quantum corrections to the inflaton potential that ruins its flatness, is resolved. Also, some potentials that are excluded by Cosmic Microwave Background (CMB) data in the cold inflation scenario are allowed in the warm inflation scenario (though the converse is also true). Models of warm inflation usually require a very large number of fields ($10^4 - 10^6$) to be coupled to the inflaton to maintain a thermal bath with $T > H$ [14, 15], which may be unattractive. However recently proposed warm inflation models with the inflaton as a pseudo-Nambu-Goldstone boson require only two additional fields [16, 17].

Given the importance of warm inflation, it is then important to constrain the parameters of warm inflation scenarios using Cosmic Microwave Background (CMB) data just like it is done for various cold inflation scenarios. In this work, we constrain the parameters of warm inflation driven by a quartic potential using complete Planck 2015 data (temperature, polarization and lensing). In particular, we focus on obtaining the marginal and joint probability distributions of the parameters involved in the model by carrying out a full Markov-Chain Monte Carlo analysis using `CosmoMC` [18], a publicly available code.

A quartic warm inflation model is described by the inflaton's self coupling λ and its dissipation rate to other fields described by the dissipation coefficient Υ . In the literature there are usually two forms for this dissipation coefficient, $C_T T$ and $C_\phi T^3/\phi^2$. Here we consider only the latter form, which is obtained from inflaton decay to lighter particles mediated by heavier particles ($T > m$) [19–21] and C_ϕ is related to the inflaton couplings and the multiplicities of other fields in the model. More generally, $\Upsilon = CT^c\phi^{2a}/M_X^{2b}$ with $c + 2a - 2b = 1$ [22], where M_X is the mass of the intermediate particle. For a model builder, knowing constraints from the data on λ and C_ϕ will be very useful.

The power spectrum for quartic warm inflation depends on λ, C_ϕ and ϕ_k , where the subscript k indicates that quantities are evaluated at the time when the scale k crosses the horizon during inflation. In the literature on warm inflation, the authors have introduced the variable $Q = \Upsilon/(3H)$. The power spectrum for quartic chaotic warm inflation then effectively depends on λ, Q_k and N_k , the number of e-foldings of inflation from the end of inflation to the epoch when the scale k crosses the horizon. [Recall that in cold inflation the power spectrum can be made to be effectively dependent on λ and N_k (see, for example, Eq. (8.71) of Ref. [23] for quartic chaotic inflation).]

For cold inflation, the normalisation of the power spectrum at the pivot scale k_P fixes the value of λ , for a fixed N_P , where P indicates that quantities are evaluated at the time when the pivot scale k_P crosses the horizon during inflation. We find that in warm inflation too fixing the normalisation at the pivot scale fixes the value of λ for fixed N_P and a particular value of Q_P . We find that for the scales of cosmological interest the power spectrum is close to power law, and we study the dependence of the primordial power spectrum on the parameters of the model. We then study the angular power spectrum using the publicly available code `CAMB` [37] and finally constrain the parameters of the quartic warm inflation model using `CosmoMC`. In our analysis, we fix N_P to be either 50 or 60.

We begin by summarizing the known results about the primordial power spectrum in warm inflation. We then express the primordial power spectrum for the warm inflation model with a quartic potential as a function of λ, C_ϕ and Q_P , and then eventually in terms of λ, Q_P and N_P . We discuss features of the power spectrum and correlations between parameters of the model. Thereafter we present our Monte-Carlo Markov Chain analysis using `CosmoMC` for which we use the full Planck 2015 data (high- l TT, TE, TE + low- l polarization + lensing) for our analysis. We explain how we constrain the parameters of quartic warm inflation

and finally show the obtained joint and marginal probability distributions of λ and Q_P . We provide the mean and standard deviation for these parameters and highlight the degeneracy between the parameters.

2 Evolution equations in warm inflation

For the inflaton ϕ interacting with other fields the evolution is governed by

$$\ddot{\phi} - \nabla^2 \phi + 3H\dot{\phi} + \Upsilon\dot{\phi} + V' = (2\Upsilon T)^{\frac{1}{2}}\xi(x, t), \quad (2.1)$$

where, H is the Hubble parameter during inflation, the overdots are derivatives w.r.t. cosmic time, prime indicates the derivative w.r.t. ϕ , Υ is the inflaton dissipation rate and ξ represents stochastic fluctuations due to interactions of ϕ with other species. The stochastic r.h.s and the dissipation rate on the l.h.s are related through the fluctuation-dissipation theorem [22, 24, 25]. For the background homogeneous field $\phi(t)$, and a zero mean for $\xi(t)$

$$\ddot{\phi} + 3H\dot{\phi} + \Upsilon\dot{\phi} + V' = 0. \quad (2.2)$$

Recall that for a damped harmonic oscillator, $\ddot{x} + 2b\dot{x} + \omega^2 x = 0$, and the friction term, i.e. $2b\dot{x}$, causes dissipation and non-conservation of energy. Moreover, the rate of loss of energy is given by $dE/dt = -b\dot{x}^2$. Similarly, during warm inflation, for the scalar field we have [26]

$$\dot{\rho}_\phi + 3H(\rho_\phi + p_\phi) = -\Upsilon\dot{\phi}^2, \quad (2.3)$$

where $\Upsilon\dot{\phi}^2$ is the rate at which the inflaton loses energy. Dissipation causes radiation to be produced and the radiation energy density ρ_r evolves as

$$\dot{\rho}_r + 4H\rho_r = \Upsilon\dot{\phi}^2. \quad (2.4)$$

Assuming the radiation thermalises quickly, the radiation energy density and temperature are related by

$$\rho_r = (\pi^2/30)g_*T^4, \quad (2.5)$$

where, T is the temperature of the radiation bath and g_* is the number of relativistic degrees of freedom during warm inflation. The notion of thermal equilibrium and a temperature is only valid for $T_k > H_k$, as the Hubble radius H_k^{-1} is then greater than the thermal de Broglie wavelength $\sim T_k^{-1}$ [27]. This then gives a lower bound on Q_P , as we discuss later.

The various different realizations of warm inflation lead to different dependences of Υ on the temperature. Here we focus on the models of warm inflation in which the inflaton is coupled only indirectly to light fields ($m < T$) through heavy mediator fields ($m > T$). (Direct coupling of light fields to the inflaton gives large thermal corrections to the potential thereby spoiling its flatness and effectively leading to too few e-foldings of inflation [28, 29].) Then one finds that [19–21]

$$\Upsilon(\phi, T) = C_\phi \frac{T^3}{\phi^2}, \quad (2.6)$$

where C_ϕ is a dimensionless constant. Typically, in supersymmetric models such as the ones considered in Ref. [21, 27] one gets

$$C_\phi = \frac{h^2}{16\pi} N_X N_Y, \quad (2.7)$$

where N_X and N_Y are the number of heavy mediator fields and light fields respectively and h is a Yukawa coupling. Note that for a small effective Yukawa coupling of $h\sqrt{N_Y}$ there can be a large contribution to Υ from dissipation to on shell heavy mediator particles, that later decay to Y particles, due to a narrow resonance that overcomes the Boltzmann suppression [21].

In the slow roll approximation, one can ignore the $\ddot{\phi}$ term, and the background field evolution equation gives

$$\dot{\phi} \approx \frac{-V'(\phi)}{3H(1+Q)}, \quad (2.8)$$

where Q is defined by

$$Q = \frac{\Upsilon(\phi, T)}{3H(t)}. \quad (2.9)$$

Similarly, ignoring $\dot{\phi}^2$ as compared to $V(\phi)$, and the sub-dominant ρ_r , Einstein's equation implies that

$$H^2 = \frac{8\pi}{3} \frac{V(\phi)}{M_{Pl}^2}, \quad (2.10)$$

where $M_{Pl} = 1/\sqrt{G} = 1.2 \times 10^{19}$ GeV is the Planck mass. The slow roll parameters for warm inflation are defined as

$$\epsilon_\phi = \frac{M_{Pl}^2}{16\pi} \left(\frac{V_{,\phi}}{V} \right)^2, \quad \eta_\phi = \frac{M_{Pl}^2}{8\pi} \frac{V_{,\phi\phi}}{V}, \quad \beta_\Upsilon = \frac{M_{Pl}^2}{8\pi} \left(\frac{\Gamma_{,\phi} V_{,\phi}}{\Gamma V} \right). \quad (2.11)$$

In the literature, one also defines the Hubble flow function [30]

$$\epsilon_1 = \frac{d \ln(H_P/H)}{dN} = -\frac{\dot{H}}{H^2}. \quad (2.12)$$

The slow roll parameters and the Hubble flow function are evaluated at the pivot scale. Setting $\dot{H} = H_{,\phi} \dot{\phi}$ it is easy to verify that

$$\epsilon_1 = \frac{\epsilon_\phi}{1+Q} = \frac{1}{1+Q} \frac{M_{Pl}^2}{16\pi} \left(\frac{V'}{V} \right)^2. \quad (2.13)$$

The slow roll conditions needed for the inflationary phase are [31]

$$\epsilon_\phi \ll 1+Q, \quad |\eta_\phi| \ll 1+Q, \quad |\beta_\Upsilon| \ll 1+Q. \quad (2.14)$$

In warm inflation one presumes that $\dot{\rho}_r \approx 0$ and the temperature of the Universe is approximately unchanged. Then

$$\rho_r \approx \frac{3}{4} Q \dot{\phi}^2. \quad (2.15)$$

Figures (1) and (5) show how ρ_r and T vary with time during warm inflation. $\dot{\rho}_r \approx 0$ is valid when modes of cosmological interest cross the horizon during inflation, but it seems to be only approximately true for the entire duration of inflation. However $\dot{\rho}_r$ is small compared to the other terms in Eq. (2.4) throughout inflation and hence the approximation is valid.

3 Warm inflation model with a quartic potential

We consider a warm inflation model with a quartic potential

$$V(\phi) = \lambda\phi^4 \quad (3.1)$$

and a dissipation coefficient $\Upsilon = C_\phi \frac{T^3}{\phi^2}$. Then

$$Q = \frac{\Upsilon}{3H} = \frac{C_\phi T^3}{3H \phi^2}. \quad (3.2)$$

For a quartic potential, we get

$$H^2 = \frac{8\pi \lambda \phi^4}{3 M_{\text{Pl}}^2} \quad (3.3)$$

and the Hubble flow function

$$\epsilon_1 = \frac{1}{1+Q} \frac{1}{16\pi} \left(\frac{M_{\text{Pl}}}{\phi} \right)^2. \quad (3.4)$$

It is easy to verify that $\epsilon_\phi = \frac{2}{3}\eta_\phi = -\beta\Upsilon$.

3.1 The primordial power spectrum

The scalar primordial power spectrum is given in Ref. [27] (based on Refs. [10, 12, 22, 32, 33]) as

$$P_{\mathcal{R}}(k) = \left(\frac{H_k^2}{2\pi\dot{\phi}_k} \right)^2 \left[1 + 2n_k + \left(\frac{T_k}{H_k} \right) \frac{2\sqrt{3}\pi Q_k}{\sqrt{3+4\pi Q_k}} \right], \quad (3.5)$$

where $n(k)$ is the distribution of quanta of inflaton fluctuations $\delta\phi$ and the subscript k refers to the time when a k mode leaves the Hubble radius during inflation. Treating the inflaton field and the radiation as coupled fluids, it has been argued that perturbations in the radiation, because of inhomogeneous dissipation, can lead to a growing mode in the inflaton perturbations which causes an enhancement in the primordial power spectrum in terms of a multiplicative factor whose form depends on the form of Υ [17, 34]. For a cubic dissipation coefficient, it is obtained numerically in Ref. [42] as $G_{\text{cubic}}(Q_P) = 1 + 4.981 Q_P^{1.946} + 0.127 Q_P^{4.330}$. As our analysis is done for the weak dissipation regime, $10^{-5} < Q_P < 10^{-1}$, we can neglect it, as it is approximately 1 for the whole range of Q_P of interest to us. (For large dissipation, $Q_P \gg 1$, it was argued that inflaton perturbations can be sufficiently enhanced to make them incompatible with observations [25], but subsequently it was shown that shear viscosity in the non-equilibrium radiation damps the radiation perturbations and hence the enhancement of the inflaton perturbations.) The tensor power spectrum is given by the same expression as in cold inflation, namely,

$$P_T(k) = \frac{16}{\pi} \left(\frac{H_k}{M_{\text{Pl}}} \right)^2. \quad (3.6)$$

We wish to express the scalar and tensor power spectra as functions of k . To this end, we look at the each term appearing in Eq. (3.5) individually:

- *Prefactor*: Using Eqs. (2.8) and (3.3)

$$\frac{H_k^2}{2\pi\dot{\phi}_k} = \sqrt{\frac{8\pi}{3}} \sqrt{\lambda} \left(\frac{\phi_k}{M_{\text{Pl}}} \right)^3 (1 + Q_k). \quad (3.7)$$

- *T/H term:* Using the expression for $\rho_r(T)$ in Eq. (2.15), and Eqs. (2.8), (3.1) and (3.3) we get

$$T_k = \left(\frac{15}{\pi^3 g_*} \frac{Q_k}{(1+Q_k)^2} \lambda \phi_k^2 M_{\text{Pl}}^2 \right)^{\frac{1}{4}}. \quad (3.8)$$

Furthermore from Eq. (3.3) we obtain ¹

$$\frac{T_k}{H_k} = \left(\frac{15}{\pi^3 g_*} \right)^{\frac{1}{4}} \sqrt{\frac{3}{8\pi}} \lambda^{-\frac{1}{4}} \frac{Q_k^{\frac{1}{4}}}{(1+Q_k)^{\frac{1}{2}}} \left(\frac{\phi_k}{M_{\text{Pl}}} \right)^{-\frac{3}{2}}. \quad (3.9)$$

- *Occupation number:* We take the inflaton distribution, n_k , to be represented by a Bose-Einstein distribution,

$$n_k = \frac{1}{\exp(\frac{k/a_k}{T_k}) - 1} \quad (3.10)$$

where a is the scale factor and T represents the physical temperature. Then the first two terms in the square bracket of Eq. (3.5) become

$$1 + 2n_k = \coth \frac{H_k}{2T_k}, \quad (3.11)$$

with H_k/T_k obtained from Eq. (3.9). If $n_k = 0$ then

$$1 + 2n_k \rightarrow 1. \quad (3.12)$$

We discuss the importance of the coth term in Sec. §5.2.

The above discussion implies that the scalar power spectrum in Eq. (3.5) depends on λ , Q_k and ϕ_k . Furthermore, using the slow roll equations, Eqs. (2.8) and (2.15), and Eq. (2.6) for T , one can express Q_k as a function of ϕ_k . This can then be inverted to give ϕ_k in terms of Q_k , as in Eq. (21) of Ref. [35], as ²

$$\left(\frac{\phi_k}{M_{\text{Pl}}} \right) = \sqrt{\frac{1}{8\pi}} \left(\frac{64C_\phi^4 \lambda}{9C_R^3} \frac{1}{Q_k(1+Q_k)^6} \right)^{\frac{1}{10}}, \quad (3.13)$$

where $C_R = (\pi^2/30)g_*$.

3.2 Obtaining the dissipation parameter Q_k

In order to obtain the k dependence of the scalar power spectrum, we need to find the k dependence of Q_k . From Eq. (13) of Ref. [27] (based on Ref. [35]) we have ³

$$\frac{dQ}{dN} = -\frac{1}{C_1} \frac{Q^{6/5}(1+Q)^{6/5}}{1+7Q}, \quad (3.14)$$

¹We note that Eq. (27) of Ref. [35] gives another expression for T_k/H_k , which we do not use (it can be obtained by multiplying Eqs. (3.3) and (2.9), and then using Eq. (2.6) on the r.h.s.).

²Note that our λ is equivalent to λ^2 in Ref. [35].

³Our expression for dQ/dN differs from that in Ref. [27] by a minus sign because our N is measured from the end of inflation.

where $N = \ln(a_e/a)$ is the number of e-foldings of inflation from the end of inflation, and

$$C_1 = \frac{1}{40} \left(\frac{64C_\phi^4 \lambda}{9C_R^3} \right)^{\frac{1}{5}}. \quad (3.15)$$

In order to find the k dependence, it is useful to define $x = \ln(k/k_P)$. Then,

$$\frac{dQ}{dx} = \frac{dQ}{dN} \frac{dN}{dx}. \quad (3.16)$$

Since $N = \ln(a_e/a)$ and $a = k/H$, $dN/dx = -1 + H^{-1}dH/dx = -1 + H^{-1}(dH/dN)(dN/dx)$. Then using $\epsilon_1 = H^{-1}dH/dN$, we get

$$\frac{dN}{dx} = -\frac{1}{1 - \epsilon_1}. \quad (3.17)$$

Therefore

$$\frac{dQ}{dx} = \frac{1}{[1 - \epsilon_1]} \frac{1}{C_1} \frac{Q^{6/5}(1+Q)^{6/5}}{1+7Q}. \quad (3.18)$$

One integrates the above equation from the time when k^{th} mode leaves the horizon till when the pivot scale crosses the horizon to get a relation between Q_k and k in the form of a transcendental equation as

$$G(Q_k) - G(Q_P) = x, \quad (3.19)$$

where

$$G(Q) = \frac{C_1}{12Q^{1/5}(1+Q)^{6/5}} \left[-32 \left(\frac{10125\pi^6 Q(1+Q)^6}{C_\phi^4 \lambda} \right)^{1/5} \ln(Q(1+Q)^6) + 15(1+Q) \left(-4 + 20Q - 15Q(1+Q) {}_2F_1 \left(1, \frac{8}{5}, \frac{9}{5}, -Q \right) \right) \right] \quad (3.20)$$

and ${}_2F_1(a, b, c, z)$ is the Hypergeometric function.

Combining Eqs. (3.19) and (3.20) with the expressions in Sec. §3.1 we can express the power spectrum $P_{\mathcal{R}}$ as a function of k , and the parameters λ, C_ϕ and Q_P .

3.3 Duration of inflation

We have to ensure that the parameters we choose for the power spectrum correspond to a scenario that gives sufficient e-foldings of inflation. Applying the condition that inflation lasts for N_P e-foldings after the pivot scale crosses the horizon during inflation provides a relation between the parameters λ and C_ϕ . Integrating Eq. (3.14) from the time when k^{th} mode leaves the horizon till when the pivot scale crosses the horizon we get ⁴

$$N_k - N_P = C_1 [F(Q_P) - F(Q_k)], \quad (3.21)$$

⁴ Note that C_1 is referred to as C_Q in Ref. [35] and $1/C_Q$ in Ref. [26] while $1/C_1$ is C_* in Ref. [27] which is approximated as $C_1^{-1} = C_* \approx 5\epsilon_k Q_k^{-1/5}$ for $Q_k \ll 1$, where ϵ_k is a k dependent slow roll parameter. (On substituting the definition of ϵ_ϕ , $C_* = 5\epsilon_\phi Q_P^{-1/5} = 5M_{Pl}^2/16\pi(V'/V)_P^2 Q_P^{-1/5} = 40 \left(\frac{M_{Pl}}{\sqrt{8\pi\phi_P}} \right)^2 Q_P^{-1/5}$. Using Eq. (3.13), this is equal to $40 \left(\frac{9C_R^3 Q_P (1+Q_P)^6}{2^6 C_\phi^4 \lambda} \right)^{2/10} Q_P^{-1/5} = 40 \left(\frac{9C_R^3}{2^6 C_\phi^4 \lambda} \right)^{1/5} (1+Q_P)^{6/5} \approx 40 \left(\frac{9C_R^3}{2^6 C_\phi^4 \lambda} \right)^{1/5} = \frac{1}{C_1}$ for $Q_P \ll 1$. Hence C_* is independent of k for $Q_P \ll 1$.)

where C_1 is as given in Eq. (3.15) and

$$F(Q) = \frac{5}{4Q^{\frac{1}{5}}(1+Q)} \left[4(1+Q)^{\frac{4}{5}}(-1+5Q) - 15Q(1+Q) \cdot {}_2F_1\left(\frac{1}{5}, \frac{4}{5}, \frac{9}{5}, -Q\right) \right], \quad (3.22)$$

where again ${}_2F_1(a, b, c, z)$ is the Hypergeometric function.⁵

Let us consider the mode which crosses the Hubble radius at the end of inflation. For such a mode $N_k = 0$ and Eq. (3.21) implies that

$$N_P = C_1[F(Q_e) - F(Q_P)]. \quad (3.23)$$

We can obtain Q_e by setting the second potential slow roll parameter η_ϕ to $1 + Q_e$, i.e.

$$\eta_e = \frac{3}{2\pi} \frac{M_{\text{Pl}}^2}{\phi_e^2} = 1 + Q_e. \quad (3.24)$$

For the model under consideration, warm inflation ends because the slow roll conditions fail, and not because ρ_r overtakes ρ_ϕ , as seen in Figure (1), where $\rho_{\phi e} \sim 3\rho_{re}$. (Since, as shown earlier, η_ϕ is the largest slow roll parameter it is sufficient to verify the breakdown of the slow roll condition with η_ϕ .) Expressing ϕ_e in terms of Q_e using Eq. (3.13) we get

$$Q_e^2 + Q_e - \left(\frac{64C_\phi^4\lambda}{9C_R^3} \right) \frac{1}{12^5} = 0, \quad (3.25)$$

whose positive solution is

$$Q_e = \frac{-1 + \sqrt{1 + 4 \left(\frac{64C_\phi^4\lambda}{9C_R^3} \right) \frac{1}{12^5}}}{2}. \quad (3.26)$$

Notice that Q_e depends on λC_ϕ^4 .

Using the expressions for C_1 (Eq. (3.15)) and Q_e (Eq. (3.26)) in Eq. (3.23), we get a value for λC_ϕ^4 for a given value of N_P and Q_P which we can use to express C_ϕ in terms of λ . Using this in $P_{\mathcal{R}}(k)$ the parameters defining the power spectrum are now λ , Q_P and N_P . Similarly one can obtain the tensor power spectrum $P_T(k)$ in terms of these parameters. By choosing the value of N_P appropriately to be, say 50 or 60, we can ensure that we have a sufficient duration of inflation.

Thus, the above implies that it is the values of λ , Q_P and N_P that need to be constrained from the CMB observational data. Therefore in our `CosmoMC` code we vary the parameters λ and Q_P while keeping N_P fixed for a particular run.

As an aside we note that,

$$\begin{aligned} N_k &= \ln \frac{a_e}{a_k} = \ln \frac{a_e}{a_P} + \ln \frac{a_P}{a_k} \\ &= N_P + \ln \left(\frac{k_P}{k} \frac{H_k}{H_P} \right) \\ &= N_P + \ln \frac{k_P}{k} + \ln \frac{\phi_k^2}{\phi_P^2}, \end{aligned} \quad (3.27)$$

⁵Note that our $F(Q)$ is different from $F_r(Q)$ in Eq. (26) of Ref. [35]. We are unable to reproduce Eq. (25) of Ref. [35].

which, using Eq. (3.13), gives

$$N_k - N_P = -\ln \frac{k}{k_P} + \ln \left[\frac{Q_P(1 + Q_P)^6}{Q_k(1 + Q_k)^6} \right]^{\frac{1}{5}}. \quad (3.28)$$

Combining Eqs. (3.21) and (3.28) then gives us Q_k as a function of $\ln(k/k_P)$, for a given Q_P and N_P . We have numerically confirmed that this agrees with the $Q_k(x)$ that we obtain from Eqs. (3.19) and (3.20). In our numerical code we use Eqs. (3.19) and (3.20).

4 Primary analysis using the primordial power spectrum and its normalisation

In the last section we argued that the primordial power spectrum is completely determined by the values of the three parameters N_P , Q_P and λ . These will be the parameters we vary when we perform a detailed data analysis with `CosmoMC`. But before presenting those results, we shall study using `Mathematica` the power spectrum and understand how these parameters determine various features of the quartic model under consideration. For this section we also impose the normalisation of the power spectrum as $P_{\mathcal{R}}(k_P) \equiv A_s = 2.2 \times 10^{-9}$. For any given value of Q_P and N_P this constraint then fixes λ .⁶ To appreciate how parameters change during warm inflation we also plot the homogeneous inflaton field ϕ , Q_k and the energy density of ϕ and the radiation as a function of the number of efoldings of inflation in Figure (1).

4.1 Spectral index

We first plot the power spectrum for different values of Q_P while keeping N_P fixed at 50 and A_s fixed as above. This is shown in Figure (2), along with the standard power law power spectrum with n_s equal to the mean value of 0.9653 obtained by the Planck collaboration with TT, TE, EE + low P + lensing 2015 data [36]. The different plots for warm inflation correspond to different values of λ , chosen appropriately to give the correct normalisation A_s . It is noteworthy that as we decrease Q_P from 10^{-1} to $10^{-2.2}$, the slope of the power spectrum decreases, and then increases as we further decrease Q_P to 10^{-5} . This behaviour is best understood by studying the dependence of n_s on Q_P in Figure (3). It is also worth noting from Figure (3) that for none of the values of Q_P in the range we shall study will the power spectrum fall on top of the standard power law spectrum (the solid line in Figure (2)).

One can determine the scalar spectral index as

$$n_s - 1 \equiv \left. \frac{d \ln P_{\mathcal{R}}(k)}{d \ln(k/k_P)} \right|_{k=k_P} = \frac{d \ln P_{\mathcal{R}}}{d Q_k} \left. \frac{d Q_k}{d \ln(k/k_P)} \right|_{k=k_P}. \quad (4.1)$$

We obtain the first derivative by expressing $P_{\mathcal{R}}(k)$ in terms of Q_k using Eqs. (3.5,3.7,3.9,3.11) and (3.13) and then by taking the derivative w.r.t. Q_k . $\frac{d Q_k}{d \ln(k/k_P)}$ is given in Eq. (3.18). Then the scalar spectral index can be written as

⁶For our subsequent `CosmoMC` analysis we prefer λ , Q_P and N_P as the independent parameters as λ is more fundamental to the model than A_s .

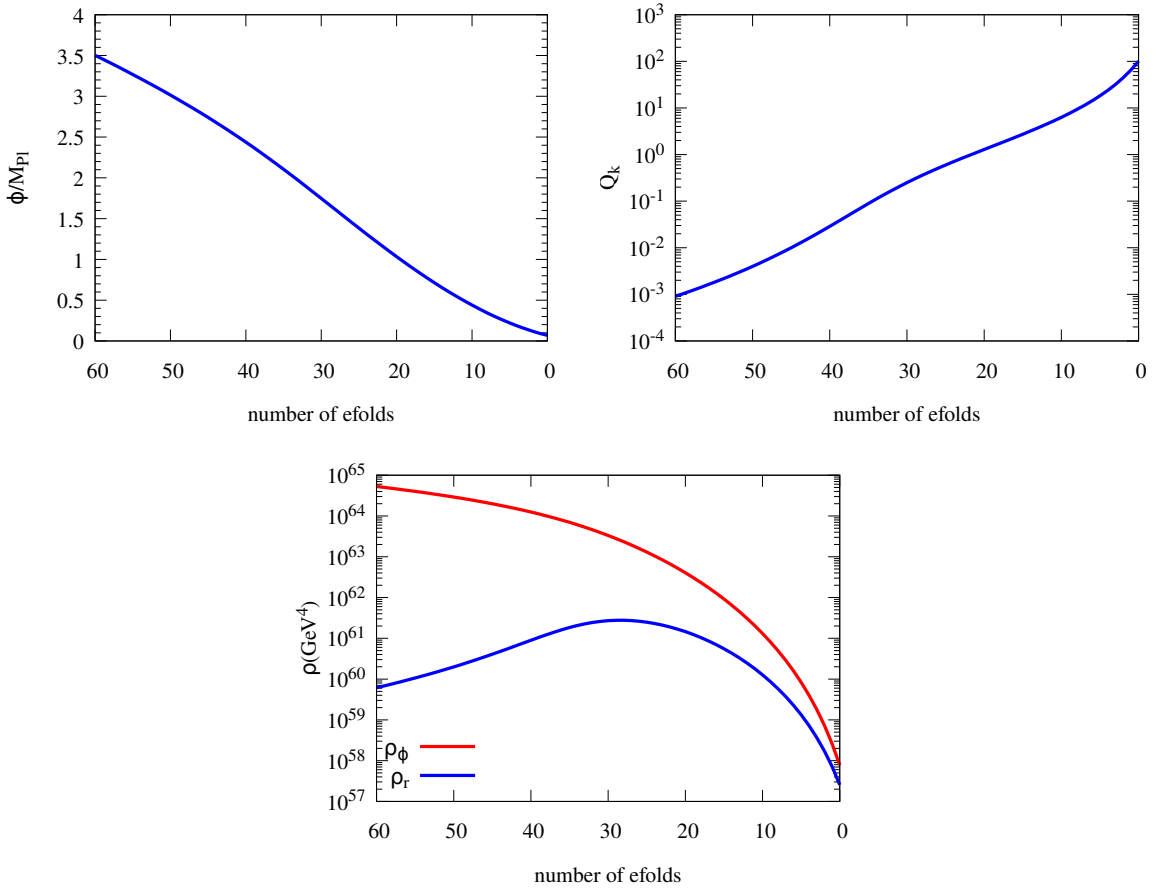


Figure 1. The behaviour of the homogeneous inflaton field ϕ , Q_k , and the energy density in ϕ and radiation is shown as a function of the number of e-foldings N . Note that as Q crosses 1 during inflation the model transits from weak dissipation to strong dissipation. For our model ρ_ϕ is larger than ρ_r till when the slow roll conditions fail and the latter therefore determines when inflation ends. Consequently the Universe will also go through a phase of reheating after inflation. All plots correspond to $N_P = 50$ and fixed A_s , and $Q_P = 10^{-2.4}$.

$$\begin{aligned}
n_s = & 1 - \frac{3\epsilon_1}{1 - \epsilon_1} + \frac{10\epsilon_1 Q_P}{(1 + 7Q_P)(1 - \epsilon_1)} \\
& + \frac{1}{(1 - \epsilon_1)} \frac{4n_P\epsilon_1}{1 + 2n_P + \delta} \left(\frac{e^{H_P/T_P}}{e^{H_P/T_P} - 1} \frac{H_P}{T_P} \right) \left(\frac{1 + 2Q_P}{1 + 7Q_P} \right) \\
& + \frac{1}{(1 - \epsilon_1)} \frac{\delta\epsilon_1}{(1 + 7Q_P)} \frac{1}{1 + 2n_P + \delta} \left[2 + 4Q_P + 5(1 + Q_P) \left(\frac{3 + 2\pi Q_P}{3 + 4\pi Q_P} \right) \right], \quad (4.2)
\end{aligned}$$

where $n_P = n(k_P)_{k_P}$ and we define $\delta = \frac{2\sqrt{3}\pi Q_P}{\sqrt{3+4\pi Q_P}} \frac{T_P}{H_P}$.

The behaviour of n_s as we change Q_P is shown in Figure (3) which explains the changes in the slope of the power spectrum seen in Figure (2). Note that the value of n_s that corresponds to the mean value of Q_P of $10^{-2.4}$, obtained by us using CosmoMC, is 0.9659 which differs slightly from the mean value of n_s of 0.9653. We also show the running of the spectral index at the pivot scale, and the running of the running, as we vary Q_P in the right

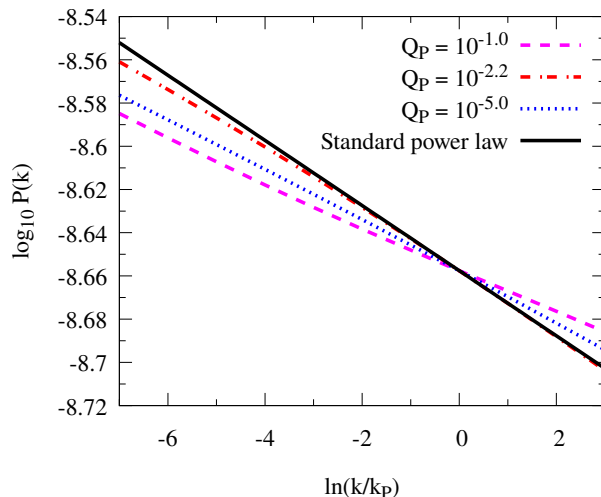


Figure 2. The primordial power spectrum, $\log_{10} P_{\mathcal{R}}(k)$ vs $\ln(k/k_p)$ is shown for different values of Q_P for $N_P = 50$ and A_s fixed. The coupling λ is different for different values of Q_P . The standard power law with $n_s = 0.9653$ is also shown as a solid (black) line.

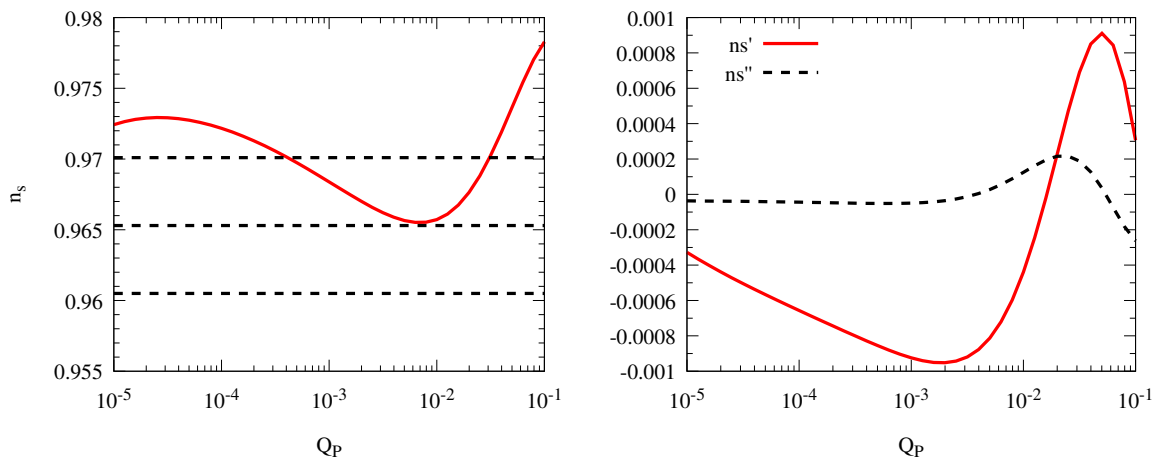


Figure 3. The behaviour of the scalar spectral index, n_s , as we change Q_P for $N_P = 50$ and A_s fixed is shown by the solid curve in the first panel. The three horizontal dashed lines show the mean value and 68 % CL limits on n_s for Planck 2015 TT, TE, EE + low P + lensing data for power law primordial power spectrum (0.9653 ± 0.0048) [36]. Note the non-monotonic behaviour of n_s . The running of the spectral index $n'_s \equiv dn_s/d(\ln k)$ and the running of the running $n''_s \equiv d^2n_s/d(\ln k)^2$ as a function of Q_P are shown in the second panel for $N_P = 50$.

panel of Figure (3) where we plot $dn_s/d(\ln k)$ and $d^2n_s/d(\ln k)^2$ as a function of Q_P for N_P fixed at 50. The extremely weak running justifies our use in Figure (3) of the allowed band of n_s values from the Planck collaboration for fixed n_s without running.

4.2 Coupling parameters λ and C_ϕ as a function of Q_P

As discussed in Sec. §3.3, N_P and Q_P determine the value of λC_ϕ^4 . For $N_P = 50$, we vary Q_P and obtain $\log_{10} \lambda C_\phi^4$ against Q_P , as shown in Figure (4). Fitting the log-log plots to a straight line, we get $\lambda C_\phi^4 = Q_P^{0.60} \times 10^{15.45}$. Imposing the normalisation A_s of the power

spectrum fixes the value of λ , as mentioned above, and we obtain λ and C_ϕ as functions of Q_P in the other panels in Figure (4). The corresponding fitting functions are $C_\phi = Q_P^{0.17} \times 10^{7.35}$ and $\lambda = Q_P^{-0.10} \times 10^{-14.0}$. This then implies $\lambda \sim C_\phi^{-0.57}$.

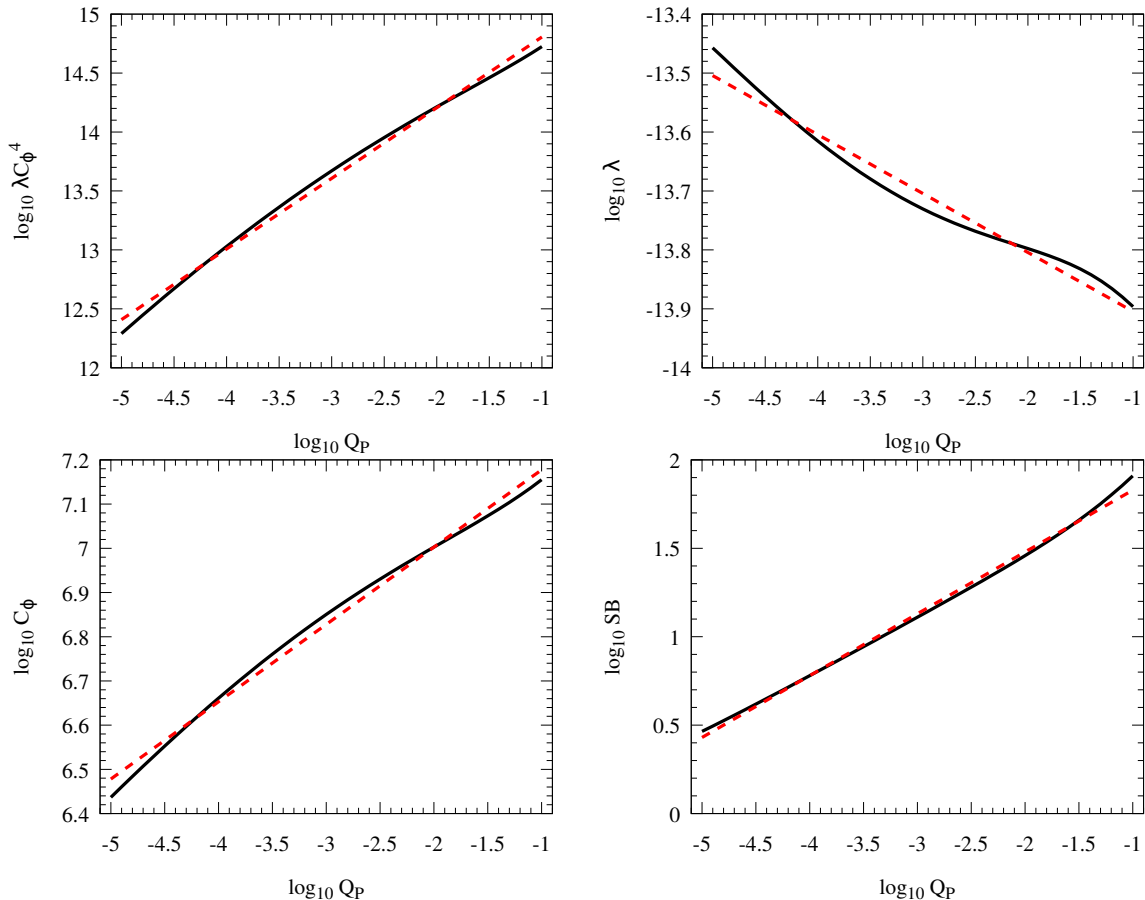


Figure 4. The first panel shows λC_ϕ^4 as a function of Q_P for $N_P = 50$. The next two panels show λ and C_ϕ as functions of Q_P for $N_P = 50$ and $A_s = 2.2 \times 10^{-9}$. The last panel shows the square bracket in Eq. (3.5) as a function of Q_P . In all the plots, the black solid curves correspond to the numerical values of the corresponding quantity and the red dashed curves are straight line fits to the log-log plots. For the first panel the fitting function is $\lambda C_\phi^4 = Q_P^{0.60} \times 10^{15.45}$, for the next two plots they are $C_\phi = Q_P^{0.17} \times 10^{7.35}$ and $\lambda = Q_P^{-0.10} \times 10^{-14.0}$, and for the final plot $SB = Q_P^{0.35} \times 10^{2.18}$.

The correlation between C_ϕ and Q_P tells us how the observational limits on Q_P , the decay width of the inflaton in units of thrice the Hubble parameter can help us estimate C_ϕ . As one can see from Eq. (2.7), C_ϕ is a function of the Yukawa coupling h and the number of mediators and light fields. As mentioned earlier, in the weak dissipation regime, the mean value of Q_P that we obtain using CMB observations is of the order of $10^{-2.4}$. The plot of C_ϕ vs Q_P in Figure (4) then indicates that the corresponding value of C_ϕ is of the order of 8.8×10^6 . For values of the Yukawa coupling in the regime of validity of perturbative calculations, this implies that $N_X N_Y$ is of order a 100 million. Thus, this implementation of warm inflation in which the inflaton couples to light degrees of freedom forming radiation through heavy mediator fields requires the existence of order 100 million fields in the corresponding microscopic theory. This requirement of a large value of C_ϕ , or a

large number of fields, has been pointed out in Ref. [14, 26, 27].

4.3 Thermal equilibrium and a lower bound on Q_P

As mentioned earlier, the temperature is defined only for $T_k > H_k$. In Figure (5), we plot T_k/H_k as a function of the number of e-foldings N for different values of Q_P , and $N_P = 50$ and fixed A_s . We find that $T_k > H_k$ holds for $Q_P > 10^{-5.0}$. One also notices that T_k/H_k increases with time till the end of inflation. We also plot T_k as a function of N . (We mention in passing that the relation between Q_P and T/H in Sec. 4 of Ref. [27] has a typographical error.)

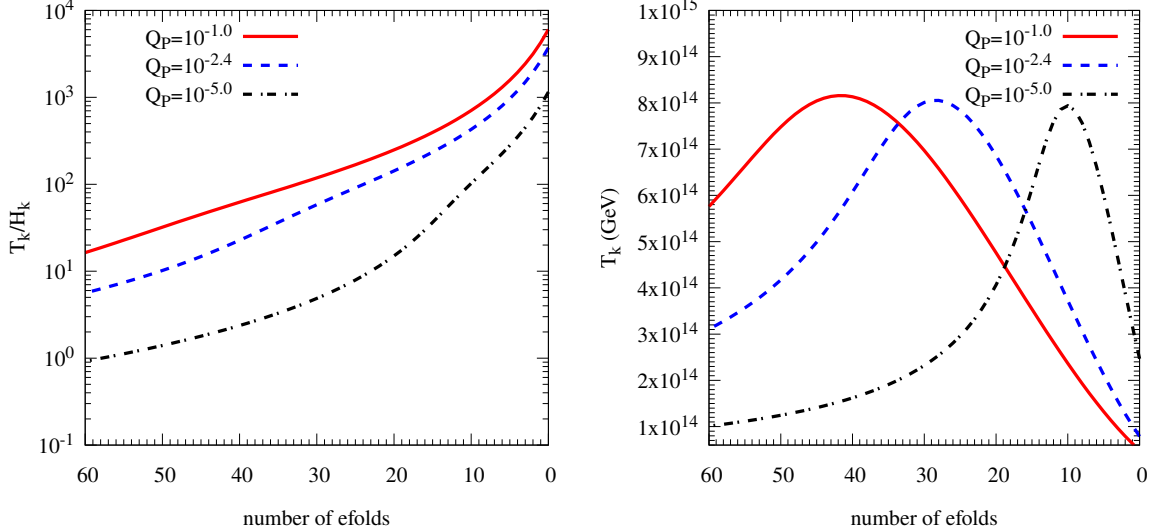


Figure 5. Plots showing T_k/H_k vs $\ln(k/k_P)$ and T_k vs $\ln(k/k_P)$ for different values of Q_P . Note that $T > H$ during inflation is valid only for $Q_P > 10^{-5}$.

4.4 Correlation between λ and Q_P

We note that for $Q_P \ll 1$ sec. §3.1 implies that

$$A_s = P_{\mathcal{R}}(k_P) \sim \lambda \left(\frac{\phi_P}{M_{\text{Pl}}} \right)^6 SB, \quad (4.3)$$

$$\sim \lambda \left(\frac{\lambda C_\phi^4}{Q_P} \right)^{\frac{6}{10}} SB, \quad (4.4)$$

where SB refers to the square bracket in Eq. (3.5). The dependence of λC_ϕ^4 on Q_P is shown in Figure (4). For $N_P = 50$ and fixed A_s we find how SB varies with Q_P , and this is also shown in Figure (4). Numerical fitting tells us that

$$\lambda C_\phi^4 \sim Q_P^{0.60}, \quad (4.5)$$

$$SB \sim Q_P^{0.35}, \quad (4.6)$$

and so

$$\begin{aligned} P_{\mathcal{R}}(k_P) &\sim \lambda \left(\frac{Q_P^{0.60}}{Q_P} \right)^{\frac{6}{10}} Q_P^{0.35}, \\ &\sim \lambda Q_P^{0.11}, \end{aligned} \quad (4.7)$$

which implies $\lambda \sim Q_P^{-0.11}$. (The factorisation of the r.h.s. of Eq. (4.7) into powers of λ and Q_P is not unique. For example, SB contains T_P/H_P which has a factor of $\lambda^{-\frac{1}{4}}$. One could try to extract it out explicitly or subsume it in the behaviour of SB as a function of Q_P , as we have done. Either way, the relation between λ and Q_P will be the same and as obtained here.)

In Sec. §4.2 we had discussed the relation between λ and Q_P for fixed A_s and N_P and found it to be $\lambda = Q_P^{-0.10} \times 10^{-14.0}$. Obviously, the fitting function between λ and Q_P must be the same no matter how it is found, and we find that the $\lambda - Q_P$ relations found earlier and in this subsection are mutually consistent, confirming our analysis. Thus, we expect that when we perform the CosmoMC analysis, we should obtain for the joint distribution of λ and Q_P a correlation between the two characterised by $\lambda \sim Q_P^{-0.1}$ for $N_P = 50$. Repeating the above analysis for $N_P = 60$ also gives $\lambda \sim Q_P^{-0.1}$ and we expect CosmoMC to give a similar result.

5 Analysis of the effects of warm inflation parameters on the CMB angular power spectrum

5.1 λ and Q_P

In Figure (6) we plot the TT angular power spectrum of CMB for fixed λ while varying Q_P , and for fixed Q_P while varying λ , respectively keeping $N_P = 50$ fixed. We obtain the plots using CAMB. We see that the angular power spectrum is sensitive to even a slight variation in λ . However it varies considerably only with order of magnitude changes in Q_P . This behaviour is also suggested by Eq. (4.7).

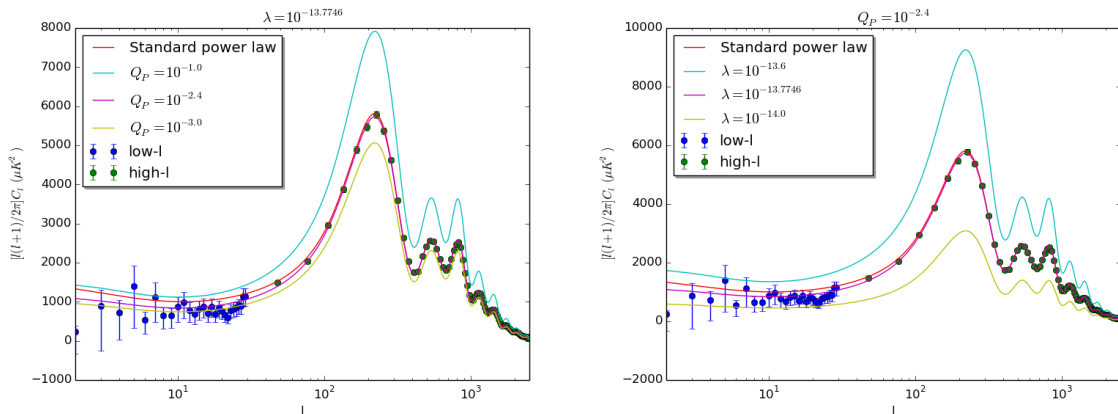


Figure 6. The plot on the left shows the TT angular power spectrum of the CMB for various values of Q_P , for λ fixed at $10^{-13.7746}$ and N_P fixed at 50. The plot on the right shows the TT angular power spectrum of CMB for various values of λ , for Q_P fixed at $10^{-2.4}$ and $N_P = 50$. For both plots, the best fit corresponds to $Q_P = 10^{-2.4}$ and $\lambda = 10^{-13.7746}$, which overlaps with the C_ℓ 's obtained with the standard power law spectrum with $n_s = 0.96$. In the plots, low ℓ refers to the range $\ell = 2 - 49$ while high ℓ refers to the range $\ell = 50 - 2500$ (see Ref. [38] for details).

5.2 Effect of the *coth* term, and a comparison with cold inflation

A Bose-Einstein distribution for inflatons has been considered in the context of cold inflation too with a similar $\text{coth}[H_k/(2T_k)]$ term [39]. In that case, it is presumed that the inflaton was

in thermal equilibrium at some early time prior to inflation, possibly at the Planck time, and subsequently its interactions froze out. Therefore one has a frozen distribution of inflatons at the beginning of inflation. Since this distribution dilutes with the expansion of the Universe, and hence during inflation, the effect of the thermal distribution is larger for larger scales. In fact, it enhances power on larger scales and if the power spectrum is pivoted at a standard pivot scale then, as seen in Fig. (1) of Ref. [39], there is excess power on large scales which requires inflation to last 7-32 more e-foldings than the standard requirement for GUT scale to electroweak scale inflation so as to dilute the effect of the inflaton distribution.

For warm inflation where one considers a thermal distribution of inflatons the distribution is replenished by dissipation and the temperature is approximately constant when cosmologically relevant k modes leave the horizon. For $N_P = 50$ and fixed A_s , and $Q_P = 10^{-2.4}$, we find that $\coth[H_k/(2T_k)]$ varies from 13 to 26 as x varies from -7 to 3 . The ratio of the square bracket SB in the primordial power spectrum with the \coth and with the \coth set to 1 varies by a factor of 13 to 17, which is also reflected in the C_ℓ 's in Figure (7), which shows the angular power spectrum for the same value of Q_P and λ with the \coth term retained and the \coth term set to 1.

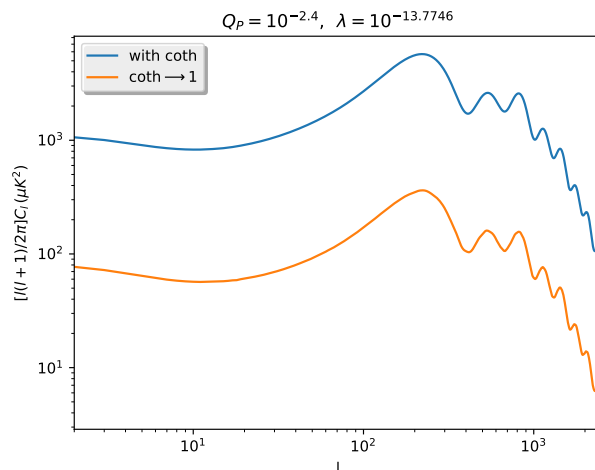


Figure 7. Angular power spectra for warm inflation for the same values of Q_P and λ are plotted using CAMB, with the \coth term retained in the primordial power spectrum for the upper blue curve and with the \coth term set to 1 for the lower orange curve. One sees that the effect of the \coth term is to enhance the angular power spectrum, and it is almost uniform across angular scales. The parameters Q_P and λ are appropriately chosen such that at the pivot scale the primordial power spectrum associated with the blue curve is normalised.

Because the \coth term shows only some variation with k , it effectively readjusts the normalisation of the prefactor in the power spectrum, i.e., it lowers H . For $N_P = 50$ and fixed A_s , and $Q_P = 10^{-2.4}$ for warm inflation, we have calculated the parameters of warm inflation with the \coth term retained, with the \coth term set to 1, and for cold inflation. The λ , ϕ_P and H_P are $(1.68 \times 10^{-14}, 3.01 M_{Pl}, 4.09 \times 10^{13} \text{ GeV})$, $(3.09 \times 10^{-13}, 3.01 M_{Pl}, 1.76 \times 10^{14} \text{ GeV})$ and $(6.14 \times 10^{-14}, 4.03 M_{Pl}, 1.40 \times 10^{14} \text{ GeV})$ respectively for the three cases. One finds that H_P for the warm inflation case with the \coth term retained is the lowest. Lower H_P lowers the tensor power spectrum and hence the tensor to scalar ratio, r , thereby making the quartic potential warm inflation scenario with the \coth term retained more compatible with Planck data. Quartic warm inflation with $n(k) = 0$, and quartic cold inflation, give too large values

of r and are incompatible with the data, as also shown in Ref. [27].

5.2.1 Recovering cold inflation

For $Q_P < 10^{-10}$ the value of λ does not change with Q_P for fixed N_P and A_s indicating that perhaps one has achieved the cold inflation limit. Indeed we find that the value of λ and n_s for $Q_P = 10^{-10}$ are 5.96×10^{-14} and 0.94 and the corresponding numbers for cold inflation are very similar at 6.14×10^{-14} and 0.94. Note that for such small Q_P , T/H is small and the coth term reduces to 1 giving a power spectrum corresponding to $n_k \approx 0$, as for standard cold inflation, which was also noted in Ref. [27].

6 Comparison with the existing literature

An analysis of the power spectrum and its dependence on the warm inflation model parameters is also given in Sec. III of Ref. [26].⁷ Their Table 3 implies that $\lambda \sim C_\phi^{-1} \sim Q_P^{-0.33}$ which differs somewhat from our result in Sec. 4.2 that $\lambda \sim C_\phi^{-0.57} \sim Q_P^{-0.1}$ for N_P equal to 50, which is corroborated by our CosmoMC analysis in Sec. §7.

In Eq. (5.23) of Ref. [40], the scalar spectral index for $Q_P \ll 1$ is given by the expression

$$n_s = 1 - 3\epsilon_1 + \frac{1}{(1 + 2n_P + \Delta_Q)} 4n_P \epsilon_1 + \frac{1}{(1 + 2n_P + \Delta_Q)} 7\epsilon_1 \Delta_Q, \quad (6.1)$$

where

$$\Delta_Q = 2\pi Q_P \frac{T_P}{H_P}.$$

We have plotted our expression for n_s in Eq. (4.2), and that in Eq. (6.1), as a function of Q_P in Figure (8) for $Q_P \leq 0.1$. One sees significant differences in the plots⁸. The expression in Ref. [40] is obtained using certain approximations and hence does not include certain factors and terms. First of all, because of the $\coth(\frac{H}{2T}) \sim \frac{T}{2H}$ for $H \ll 2T$ approximation⁹, a factor $\frac{e^{H_P/T_P} H_P}{e^{H_P/T_P-1} T_P}$ was missed by the authors. This factor varies from 1 to 1.4 as Q_P goes from 10^{-1} to 10^{-5} . Secondly, Eq. (6.1) is valid only in the $Q_P \ll 1$ approximation which is indicated by the statement just above their Eq. (5.23). If the approximation $Q_P \ll 1$ is not considered and $1 + Q_P$ is retained in the derivation, an extra term $\frac{10\epsilon_1 Q_P}{(1+7Q_P)(1-\epsilon_1)}$ is obtained as in our Eq. (4.2). This extra term is significant, $\Delta n_s \geq 0.005$, for $Q_P > 10^{-1.8}$. Thirdly, in Ref. [40] the spectral index is defined as $d \ln P_{\mathcal{R}}/dN$ instead of $d \ln P_{\mathcal{R}}/d \ln(k/k_P)$, because of which another factor of $dN/dx = -(1 - \epsilon_1)^{-1}$, as given in Eq. (3.17), is ignored¹⁰. The magnitude of this overall factor varies from 1.05 to 1.02 for Q_P between 10^{-1} to 10^{-5} . In all, the combined effect of these three factors is seen in Figure (8). In the $Q_P \ll 1$ limit, and if we drop the factor $\frac{e^{H_P/T_P} H_P}{e^{H_P/T_P-1} T_P}$, our expression for the spectral index agrees with that in Ref. [40] which implies that Eq. (6.1) is equivalent to Eq. (4.2) combined with the above approximations.

⁷ The form of the power spectrum in Eq. (30) of Ref. [26] reduces to that which we consider below in the weak dissipative limit ($Q \ll 1$) with a thermal distribution for the inflaton quanta. There is a discrepancy of a factor of 2, and terms that reduce to 1 in the small Q limit.

⁸Our analysis is for $N_P = 50$ and fixed A_s . However, if we do not fix A_s but take a fixed λ (like in Figs. 1 and 3 of Ref. [40]), one sees differences in the n_s plots obtained using Eqs. (4.2) and (6.1) similar to that in Figure (8).

⁹In Sec. 5 of Ref. [40] the argument of the coth term and the approximation for coth have typographical errors.

¹⁰In Ref. [40], dN is defined as the negative of ours and hence there is no sign discrepancy.

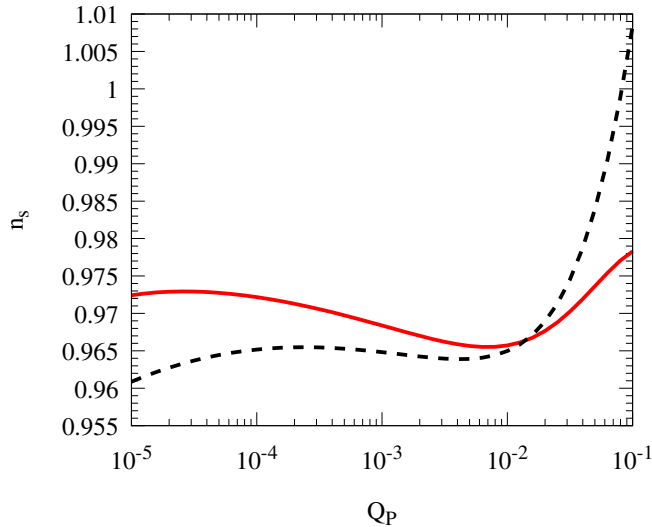


Figure 8. n_s vs Q_P from our expression in Eq. (4.2) (red solid line), and from that of Ref. [40] in Eq. (6.1) (black dashed line) for $N_P = 50$ and fixed A_s .

7 Constraining the parameters of the warm quartic chaotic inflation model with the full Planck 2015 data

As we saw in Section §3.1, for warm inflation driven by a single scalar field with a quartic self-interaction potential, for a given N_P the parameters which determine the underlying microphysics can be chosen to be Q_P and λ . We therefore obtain the joint and marginal distributions of these parameters and constrain their values.

It is well known that in cold inflation driven by a quartic potential, the self coupling λ is quite small ($\mathcal{O}(10^{-14})$). From our preliminary analysis with CAMB we have found that λ for warm inflation is similarly small. Hence we work with $-\log_{10} \lambda$ rather than λ as one of the variables in performing our analysis. In the weak dissipative regime $Q_P \ll 1$ and we use $-\log_{10} Q_P$ as another variable. We can now attempt to constrain $-\log_{10} \lambda$ and $-\log_{10} Q_P$ for the two choices of N_P i.e. $N_P = 50$ and $N_P = 60$.

For $N_P = 50$ and 60 , we use 10^{-14} to 10^{-13} and $10^{-14.5}$ to $10^{-13.5}$ respectively as the range of values for λ . The angular power spectrum is sensitive to λ and we have to choose a narrow range. As discussed in Section §4.3 for the values of Q_P smaller than 10^{-5} , one has $T < H$ and so this regime can not be thought of as a realisation of warm inflation. Keeping this in mind, we would like to consider Q_P between 10^{-5} and 10^{-1} . However for numerical reasons we consider $-\log_{10} Q_P$ between 5.4 and 1 for both $N_P = 50$ and 60 .

In the Planck 2015 likelihood analysis [41] the CMB angular power spectra at low- l are computed following a Gibbs sampling approach called COMMANDER. At high- l , the TT, TE and EE power spectra are computed by using the code Plik which computes “Pseudo-Cls” by cross-correlating the data from different frequency maps. Plik has a large number nuisance parameters, representing the foreground, calibration, etc., for computing likelihood. Although the parameters of Plik also can be estimated from the Planck 2015 data in a CosmoMC analysis we have decided not to do that and fixed their values to be the best fit values for the standard Λ CDM baseline model as given by the Planck collaboration. We carry out our MCMC search in a six dimensional parameter space with the standard parameters $\Omega_b h^2, \Omega_c h^2, \theta, \tau$, and our parameters $-\log_{10} \lambda$ and $-\log_{10} Q_P$. $\Omega_b h^2, \Omega_c h^2, \theta$ and

τ represent the baryon density, cold dark matter density, the ratio of the size of the sound horizon at decoupling (r_{dec}) and the angular diameter distance at decoupling (D_A), and the Thomson scattering optical depth due to reionization respectively. The priors for the standard parameters are found by comparing the CMB angular power spectra for a set of trial values with the observational data points using CAMB. We consider flat priors for all these parameters. We use the November 2016 version of CAMB and the July 2015 version of CosmoMC and set the flags, `compute_tensor=T`, `CMB_lensing=T`, and `use_nonlinear_lensing=F`. We use as the pivot scale $k_P = 0.05 \text{Mpc}^{-1}$, set the number of massless neutrino species to its value in the Standard Model i.e. $n_\nu = 3.046$ and similarly set the value of the Helium fraction $Y_{He} = 0.24$ in our analysis.

We present the mean and 68 % limits for the six parameters we consider in Table 1. The mean values of λ for $N_P = 50$ and 60 are 1.6×10^{-14} and 1.0×10^{-14} respectively, and of Q_P are 3.7×10^{-3} and 4.4×10^{-3} respectively. We also show the marginalized probability distributions and the joint probability distribution of these parameters in Figure (9). We find that both the parameters of the quartic warm inflation model that we consider, λ and Q_P , are well constrained by the Planck 2015 temperature and polarization data. The shape of the joint probability distribution of $-\log_{10} \lambda$ and $-\log_{10} Q_P$ in Figure (9) is best understood by comparing with the $\log_{10} \lambda$ vs $\log_{10} Q_P$ plot in Figure (4), and is consistent with the empirical relation $\lambda \sim Q_P^{-0.1}$ for $N_P = 50$ and 60 obtained in Section §4.4.

S. No.	Parameter	Priors	$N_P = 50$	$N_P = 60$
1	$\Omega_b h^2$	(0.005,0.1)	0.02220 ± 0.00013	0.02226 ± 0.00013
2	$\Omega_c h^2$	(0.001,0.99)	0.1191 ± 0.0010	0.1177 ± 0.0009
3	100θ	(0.50,10.0)	1.04089 ± 0.00029	1.04105 ± 0.00029
4	$-\log_{10} \lambda$	(13.0,14.0),(13.5,14.5)	13.783 ± 0.051	13.998 ± 0.037
5	$-\log_{10} Q_P$	(1.0,5.4)	2.4358 ± 0.5856	2.3585 ± 0.4495
6	τ	(0.1,0.8)	0.065 ± 0.011	0.075 ± 0.011

Table 1. From the Planck 2015 TT, TE, EE + low P + lensing data mean and 68% limits for the four standard and two extra parameters of the quartic model of warm inflation for 50 and 60 number of e-foldings is displayed. The priors for various parameters are also included. (For $-\log_{10} \lambda$ separate priors for $N_P = 50$ and 60 are indicated.)

A CosmoMC analysis of warm inflation for different potentials was carried out in Ref. [42]. In that analysis the CosmoMC parameters are $\Omega_c h^2$, $\Omega_b h^2$, θ , τ and Q_P , for fixed N_P . The normalization of the power spectrum at the pivot scale is also taken to be fixed. In the power spectrum, the authors parametrize Q_k , T_k/H_k and the prefactor in the power spectrum, $P_0(k) = [H_k^2/(2\pi\dot{\phi}_k)]^2$, as $a_i k^{b_i+c_i \ln(k)}$ with i referring to Q_k , T_k/H_k and $P_0(k)$ ¹¹. For each value of Q_P , and fixed $P_{\mathcal{R}}(k_P)$ and N_P , their background equations [Eqs. (2.1-2.3, 2.9-2.15)] are used to (uniquely) determine a_i, b_i and c_i . With the values of these coefficients $P_{\mathcal{R}}(k)$ is known, which is used by CosmoMC. CosmoMC then provides a likelihood curve for Q_P , as shown in their Fig. 8. The algorithm BOBYQA (Bound Optimization BY Quadratic Approximation) is used to find the best fit value. Furthermore they obtain n_s, n'_s and n''_s at k_P using their Eqs. (2.23-2.25). Planck 2015 results suggest a lower value of the tensor to scalar r , and a positive value of the running of the running parameter n''_s (albeit of small

¹¹R. Ramos, private communication.

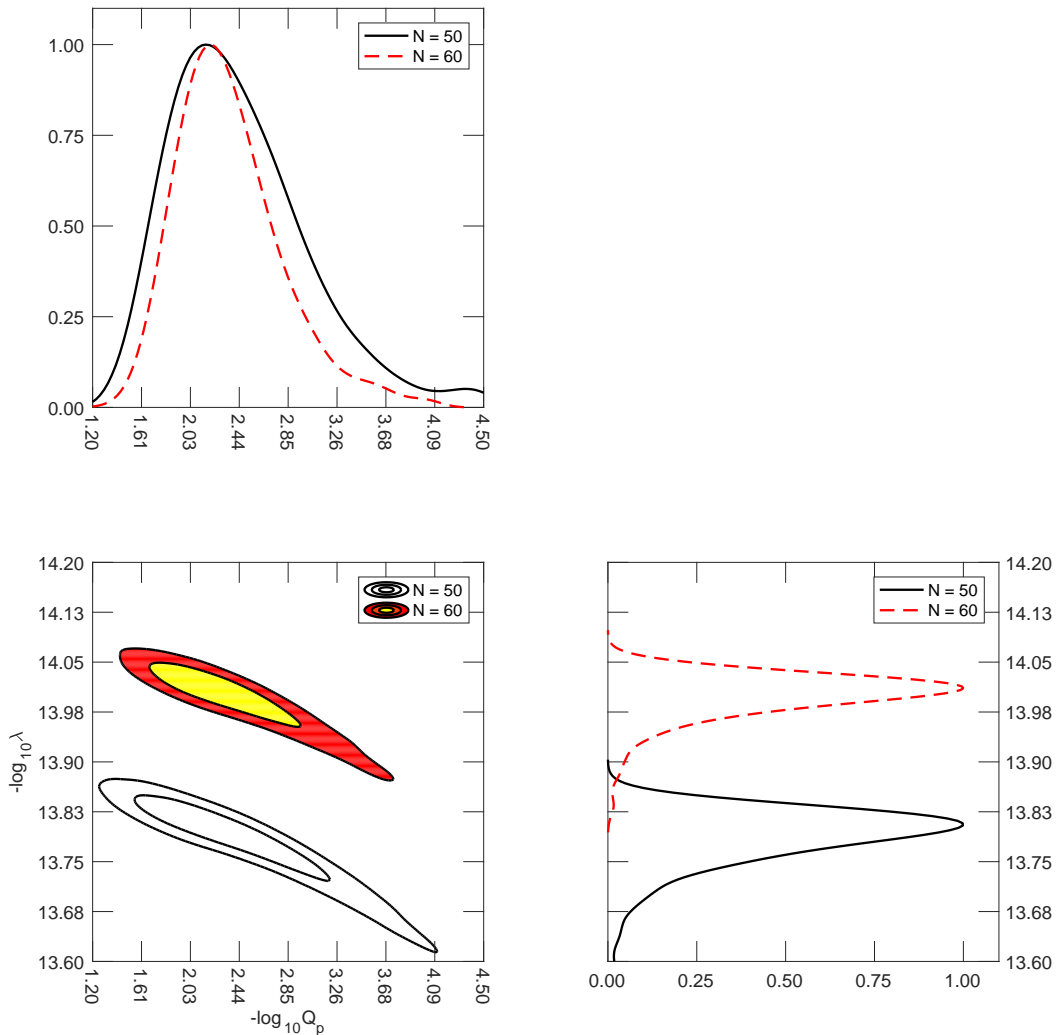


Figure 9. The joint probability distribution and the marginalized distributions for λ and Q_p . For the marginalized distributions the black solid lines are for $N_P = 50$ and the red dashed lines are for $N_P = 60$. In the contour plots of the joint probability distributions the lower contours are for $N_P = 50$ and the upper ones are for $N_P = 60$.

statistical significance) and these cannot be explained in the standard cold inflation scenario driven by a quartic potential. In Ref. [42] it has been shown that different warm inflation models can explain these features, though not quartic warm inflation.

In the present work, instead of restricting our attention to finding only the best fit value of Q_p (and then the other derived parameters), we vary both Q_p and λ . This allows us to get the joint probability distribution for the two parameters which describe the underlying microphysics of the quartic chaotic warm inflation model. Furthermore, we do the full `CosmoMC` and not just `BOBYQA`. This allows us to get the mean values and standard deviations. In algorithms such as those followed in `CosmoMC` the range of preferred values, represented by the mean and standard deviation, carry more information than the best fit value.

8 Discussion and Conclusions

The standard cold inflation is based on the simple picture in which the inflaton does not experience any dissipative dynamics as it slowly rolls down during the inflationary phase. On the other hand, warm inflation provides an example of an alternative picture, in which the dissipative dynamics plays a major role even during slow roll. The next generation CMB experiments will provide unprecedentedly stringent constraints on the various parameters characterizing the primordial power spectrum of large field inflationary scenarios [43, 44]. Given this, it is important to understand how these constraints are to be interpreted, i.e. what will these constraints teach us about the epoch of cosmic inflation. Keeping this future prospect in mind, one must first best understand how the current available data constrains the possibility of warm inflation.

In this work, we studied warm inflation driven by a scalar field with a quartic potential in the weak dissipative regime i.e. in the regime in which the inflaton decay rate is small as compared to the Hubble parameter when the modes of cosmological interest cross the horizon during inflation. We focused on constraining all aspects of this specific scenario using the most recent CMB observational data. In particular we found the joint probability distribution of λ , the self coupling of the inflaton, and Q_P , the ratio of the inflaton decay width and (three times) the Hubble parameter during inflation, evaluated at the pivot scale (0.05 Mpc^{-1}). We also found the mean and standard deviation values of these parameters. Q_P is also related to C_ϕ , a parameter related to the inflaton coupling to other fields and the number of other fields in the warm inflation model.

From the marginalised distributions of the parameters of the model we find that the preferred range of values of λ is 1.5×10^{-14} to 1.9×10^{-14} with a mean value of 1.6×10^{-14} for the number of e-foldings of inflation after the pivot scale crosses the horizon during inflation, N_P , equal to 50, and the preferred range of values for N_P equal to 60 is 9.2×10^{-15} to 1.1×10^{-14} with a mean value of 1.0×10^{-14} . The preferred range of values of Q_P is 9.5×10^{-4} to 1.4×10^{-2} with a mean value of 3.7×10^{-3} for N_P equal to 50, and the preferred range of values for N_P equal to 60 is 1.6×10^{-3} to 1.2×10^{-2} with a mean value of 4.4×10^{-3} . The values of C_ϕ corresponding to the mean values of Q_P are 8.7×10^6 (1.2×10^7) for N_P equal to 50 (60), from the analysis in Sec. §4.2.

From the joint probability distribution obtained using `CosmoMC`, as well as from the analysis of the power spectrum, normalised at the pivot scale, in Secs. 4.2 and 4.4, we obtain $\lambda \sim Q_P^{-0.1}$ for both $N_P = 50$ and 60, a potentially useful result for warm inflation model building.

Acknowledgements: It is a pleasure to acknowledge discussions with Arjun Berera, Mar Bastero-Gil and Rudnei Ramos about details of their work on the warm inflationary scenario. J.P. would like to thank the Navajbai Ratan Tata Trust (NRTT) for financial support. Numerical work for the present study was done on the IUCAA HPC facility.

Note: While this manuscript was being prepared, Ref. [45] appeared on the arXiv. They too consider a `CosmoMC` analysis of warm inflation. They consider an inflaton dissipation rate proportional to the temperature T , while above we consider $\Upsilon \sim T^3$.

References

- [1] A. A. Starobinsky, “A New Type of Isotropic Cosmological Models Without Singularity,” *Phys. Lett.* **91B**, 99 (1980).

- [2] D. Kazanas, “Dynamics of the Universe and Spontaneous Symmetry Breaking,” *Astrophys. J.* **241**, L59 (1980).
- [3] A. H. Guth, “The Inflationary Universe: A Possible Solution to the Horizon and Flatness Problems,” *Phys. Rev. D* **23**, 347 (1981).
- [4] A. D. Linde, “A New Inflationary Universe Scenario: A Possible Solution of the Horizon, Flatness, Homogeneity, Isotropy and Primordial Monopole Problems,” *Phys. Lett.* **108B**, 389 (1982).
- [5] A. Albrecht and P. J. Steinhardt, “Cosmology for Grand Unified Theories with Radiatively Induced Symmetry Breaking,” *Phys. Rev. Lett.* **48**, 1220 (1982).
- [6] A. A. Starobinsky, “Spectrum of relict gravitational radiation and the early state of the universe,” *JETP Lett.* **30**, 682 (1979) [*Pisma Zh. Eksp. Teor. Fiz.* **30**, 719 (1979)].
- [7] S. W. Hawking, “The Development of Irregularities in a Single Bubble Inflationary Universe,” *Phys. Lett.* **115B**, 295 (1982).
- [8] A. A. Starobinsky, “Dynamics of Phase Transition in the New Inflationary Universe Scenario and Generation of Perturbations,” *Phys. Lett.* **117B**, 175 (1982).
- [9] A. H. Guth and S. Y. Pi, “Fluctuations in the New Inflationary Universe,” *Phys. Rev. Lett.* **49**, 1110 (1982).
- [10] A. Berera and L. Z. Fang, “Thermally induced density perturbations in the inflation era,” *Phys. Rev. Lett.* **74**, 1912 (1995) [[astro-ph/9501024](#)].
- [11] A. Berera, “Warm inflation,” *Phys. Rev. Lett.* **75**, 3218 (1995) [[astro-ph/9509049](#)].
- [12] A. Berera, “Warm inflation at arbitrary adiabaticity: A Model, an existence proof for inflationary dynamics in quantum field theory,” *Nucl. Phys. B* **585**, 666 (2000) [[hep-ph/9904409](#)].
- [13] D. Lopez Nacir, R. A. Porto, L. Senatore and M. Zaldarriaga, “Dissipative effects in the Effective Field Theory of Inflation,” *JHEP* **1201**, 075 (2012) [[arXiv:1109.4192](#) [[hep-th](#)]].
- [14] A. Berera, M. Gleiser and R. O. Ramos, “A First principles warm inflation model that solves the cosmological horizon / flatness problems,” *Phys. Rev. Lett.* **83**, 264 (1999) [[hep-ph/9809583](#)].
- [15] M. Bastero-Gil, A. Berera and N. Kronberg, “Exploring the Parameter Space of Warm-Inflation Models,” *JCAP* **1512**, 046 (2015) [[arXiv:1509.07604](#) [[hep-ph](#)]].
- [16] H. Mishra, S. Mohanty and A. Nautiyal, “Warm natural inflation,” *Phys. Lett. B* **710**, 245 (2012) [[arXiv:1106.3039](#) [[hep-ph](#)]].
- [17] M. Bastero-Gil, A. Berera, R. O. Ramos and J. G. Rosa, “Warm Little Inflaton,” *Phys. Rev. Lett.* **117**, 151301 (2016) [[arXiv:1604.08838](#) [[hep-ph](#)]].
- [18] A. Lewis and S. Bridle, “Cosmological parameters from CMB and other data: A Monte Carlo approach,” *Phys. Rev. D* **66**, 103511 (2002) [[astro-ph/0205436](#)].
- [19] I. G. Moss and C. Xiong, “Dissipation coefficients for supersymmetric inflationary models,” [hep-ph/0603266](#).
- [20] M. Bastero-Gil, A. Berera and R. O. Ramos, “Dissipation coefficients from scalar and fermion quantum field interactions,” *JCAP* **1109**, 033 (2011) [[arXiv:1008.1929](#) [[hep-ph](#)]].
- [21] M. Bastero-Gil, A. Berera, R. O. Ramos and J. G. Rosa, “General dissipation coefficient in low-temperature warm inflation,” *JCAP* **1301**, 016 (2013) [[arXiv:1207.0445](#) [[hep-ph](#)]].
- [22] R. O. Ramos and L. A. da Silva, “Power spectrum for inflation models with quantum and thermal noises,” *JCAP* **1303**, 032 (2013) [[arXiv:1302.3544](#) [[astro-ph.CO](#)]].

- [23] E. W. Kolb and M. S. Turner, “The Early Universe”, *Front. Phys.* **69**, 1 (1990).
- [24] A. Berera, I. G. Moss and R. O. Ramos, “Warm Inflation and its Microphysical Basis,” *Rept. Prog. Phys.* **72**, 026901 (2009) [arXiv:0808.1855 [hep-ph]].
- [25] C. Graham and I. G. Moss, “Density fluctuations from warm inflation,” *JCAP* **0907**, 013 (2009) [arXiv:0905.3500 [astro-ph.CO]].
- [26] M. Bastero-Gil and A. Berera, “Warm inflation model building,” *Int. J. Mod. Phys. A* **24**, 2207 (2009) [arXiv:0902.0521 [hep-ph]].
- [27] S. Bartrum, M. Bastero-Gil, A. Berera, R. Cerezo, R. O. Ramos and J. G. Rosa, “The importance of being warm (during inflation),” *Phys. Lett. B* **732**, 116 (2014) [arXiv:1307.5868 [hep-ph]].
- [28] A. Berera, M. Gleiser and R. O. Ramos, “Strong dissipative behavior in quantum field theory,” *Phys. Rev. D* **58**, 123508 (1998) [hep-ph/9803394].
- [29] J. Yokoyama and A. D. Linde, “Is warm inflation possible?,” *Phys. Rev. D* **60**, 083509 (1999) [hep-ph/9809409].
- [30] D. J. Schwarz, C. A. Terrero-Escalante and A. A. Garcia, “Higher order corrections to primordial spectra from cosmological inflation,” *Phys. Lett. B* **517**, 243 (2001) [astro-ph/0106020].
- [31] I. G. Moss and C. Xiong, “On the consistency of warm inflation,” *JCAP* **0811**, 023 (2008) [arXiv:0808.0261 [astro-ph]].
- [32] L. M. Hall, I. G. Moss and A. Berera, “Scalar perturbation spectra from warm inflation,” *Phys. Rev. D* **69**, 083525 (2004) [astro-ph/0305015].
- [33] I. G. Moss, “Primordial Inflation With Spontaneous Symmetry Breaking,” *Phys. Lett.* **154B**, 120 (1985).
- [34] M. Bastero-Gil, A. Berera and R. O. Ramos, “Shear viscous effects on the primordial power spectrum from warm inflation,” *JCAP* **1107**, 030 (2011) [arXiv:1106.0701 [astro-ph.CO]].
- [35] S. Bartrum, A. Berera and J. G. Rosa, “Gravitino cosmology in supersymmetric warm inflation,” *Phys. Rev. D* **86**, 123525 (2012) [arXiv:1208.4276 [hep-ph]].
- [36] P. A. R. Ade *et al.* [Planck Collaboration], “Planck 2015 results. XIII. Cosmological parameters,” *Astron. Astrophys.* **594**, A13 (2016) [arXiv:1502.01589 [astro-ph.CO]] (Table 4).
- [37] <http://camb.info/>
- [38] P. A. R. Ade *et al.* [Planck Collaboration], “Planck 2013 results. XV. CMB power spectra and likelihood,” *Astron. Astrophys.* **571**, A15 (2014) [arXiv:1303.5075 [astro-ph.CO]].
- [39] K. Bhattacharya, S. Mohanty and R. Rangarajan, “Temperature of the inflaton and duration of inflation from WMAP data,” *Phys. Rev. Lett.* **96**, 121302 (2006) [hep-ph/0508070].
- [40] M. Bastero-Gil, A. Berera, I. G. Moss and R. O. Ramos, “Cosmological fluctuations of a random field and radiation fluid,” *JCAP* **1405**, 004 (2014) [arXiv:1401.1149 [astro-ph.CO]].
- [41] N. Aghanim *et al.* [Planck Collaboration], “Planck 2015 results. XI. CMB power spectra, likelihoods, and robustness of parameters,” *Astron. Astrophys.* **594**, A11 (2016) [arXiv:1507.02704 [astro-ph.CO]].
- [42] M. Benetti and R. O. Ramos, “Warm inflation dissipative effects: predictions and constraints from the Planck data,” *Phys. Rev. D* **95**, 023517 (2017) [arXiv:1610.08758 [astro-ph.CO]].
- [43] K. N. Abazajian *et al.* [CMB-S4 Collaboration], “CMB-S4 Science Book, First Edition,” arXiv:1610.02743 [astro-ph.CO].
- [44] J. B. Muoz, E. D. Kovetz, A. Raccanelli, M. Kamionkowski and J. Silk, “Towards a

measurement of the spectral runnings,” JCAP **1705**, 032 (2017) [arXiv:1611.05883 [astro-ph.CO]].

- [45] M. Bastero-Gil, S. Bhattacharya, K. Dutta and M. R. Gangopadhyay, “Constraining Warm Inflation with CMB data,” arXiv:1710.10008 [astro-ph.CO].